Published in final edited form as:
J Immunol. 2011 February 15; 186(4): 2643–2654. doi:10.4049/jimmunol.1002983.

B Lymphocytes Differentially Influence Acute and Chronic Allograft Rejection in Mice[1]

David J. DiLillo[*], **Robert Griffiths**[†], **Surya V. Seshan**[‡], **Cynthia M. Magro**[‡], **Phillip Ruiz**[§], **Thomas M. Coffman**[*,†], and **Thomas F. Tedder**[*,2]

[*]Department of Immunology, Duke University Medical Center, Durham, North Carolina 27710

[†]Division of Nephrology, Department of Medicine, Duke University Medical Center, Durham, North Carolina 27710

[‡]Department of Pathology and Laboratory Medicine, Weill Medical College of Cornell University, New York, New York 10065

[§]Department of Surgery and Pathology, Leonard M. Miller School of Medicine, University of Miami, Miami, Florida 33101

Abstract

The relative contributions of B lymphocytes and plasma cells during allograft rejection remain unclear. Therefore, the effects of B cell depletion on acute cardiac rejection, chronic renal rejection, and skin graft rejection were compared using CD20 or CD19 mAbs. Both CD20 and CD19 mAbs effectively depleted mature B cells, while CD19 mAb treatment depleted plasmablasts and some plasma cells. B cell depletion did not affect acute cardiac allograft rejection, although CD19 mAb treatment prevented allograft-specific IgG production. Strikingly, CD19 mAb treatment significantly reduced renal allograft rejection and abrogated allograft-specific IgG development, while CD20 mAb treatment did not. By contrast, B cell depletion exacerbated skin allograft rejection and augmented the proliferation of adoptively transferred alloantigen-specific $CD4^+$ T cells, demonstrating that B cells can also negatively regulate allograft rejection. Thereby, B cells can either positively or negatively regulate allograft rejection depending on the nature of the allograft and the intensity of the rejection response. Moreover, CD19 mAb may represent a new approach for depleting both B cells and plasma cells to concomitantly impair T cell activation, inhibit the generation of new allograft-specific Abs, or reduce preexisting allograft-specific Ab levels in transplant patients.

Introduction

The relative contributions of B lymphocytes and plasma cells during allograft rejection remain unclear since B cells perform multiple functions during immune responses. For example, terminally differentiated plasma cells can secrete pathogenic Ab. B cells also positively regulate cellular immune responses by serving as APCs, and B cells are required for optimal Ag-specific $CD4^+$ T cell expansion, memory formation, and cytokine production (1–4). B cells also provide costimulatory signals through CD80, CD86, and OX40L that are important for optimal T cell activation (5, 6). A population of regulatory B cells (B10 cells) has also been identified that negatively regulates inflammation and immune responses

[1]These studies were supported by grants AI56363 and AI057157 (to T.F.T.) and DK038108 (to T.M.C.) from the National Institutes of Health.

[2]Address correspondence to: Thomas F. Tedder, Box 3010, Department of Immunology, Room 353 Jones Building, Research Drive, Duke University Medical Center, Durham, NC 27710. Phone (919) 684-3681; FAX (919) 684-8982; thomas.tedder@duke.edu.

through the production of IL-10 (7). Adoptive transfer of regulatory B10 cells suppresses immune responses and disease in mouse models of delayed type hypersensitivity, experimental autoimmune encephalomyelitis, and lupus (7–10). Thus, B cells may carry out any or all of these functions during allograft rejection.

A variety of strategies have been employed to manipulate B cells and their Ab products during allograft rejection in humans and mice. Most studies using genetically B cell-deficient μMT mice have demonstrated that B cells and Ab are not required for acute allograft rejection in various models (11–13), while other reports indicate roles for B cells during allograft rejection (14, 15). Even when allograft-specific Ab production is not required for graft rejection, the exogenous addition of allograft-specific Ab can induce allograft damage (11, 15, 16). However, complex issues are associated with studying allograft rejection in μMT mice, where the immune system develops in the complete absence of B cells. μMT mice have decreased T cell repertoire and numbers (17, 18), a smaller spleen size (18), altered Th1/Th2 cytokine balance (19), and are missing follicular dendritic cells and macrophage subpopulations (20). For this reason, the current study has examined the contributions of B cells to allograft rejection using adult mice that were treated with mAbs to deplete B cells, but with otherwise intact immunity (21, 22).

In mice, CD20 and CD19 mAbs (23) deplete B cells *in vivo* by monocyte-mediated Ab-dependent cellular cytotoxicity (21, 22) without inducing a systemic cytokine release that could alter the function of other immune system components (3). More than 95% of mature B cells in the blood and primary lymphoid organs of C57BL/6 mice are depleted after 2 d by a single dose of mouse anti-mouse MB20-11 CD20 mAb, with the effect lasting up to eight weeks (24). CD20 mAb depletes mature, germinal center, and memory B cells, but does not affect plasma cell numbers or serum IgG levels (25). Mouse anti-human CD19 mAbs deplete B cells in human CD19 transgenic (huCD19Tg) mice that have otherwise intact immune systems (22, 26). Since B cell depletion using CD19 mAb represents a potential new therapy for transplantation, huCD19Tg mice were used in this study to directly compare an anti-human CD19 mAb with a potent anti-mouse CD20 mAb that depletes the vast majority of mature B cells. Moreover, huCD19 expression levels on mature B cells in the huCD19Tg mice used in this study are similar to human blood B cells (22), and human and mouse CD19 are expressed at similar cell surface densities (27, 28). Human CD19 expression in huCD19Tg mice also recapitulates CD19 expression by human pre-, immature, and mature B cells (26). While mouse CD19 expression is downregulated on plasma cells, CD19 is expressed on some circulating human plasma cells (29). Because of this, anti-huCD19 mAb depletes pre-B cells and mature B cells, and also reduces basal serum IgM and IgG levels in hCD19Tg mice. Anti-human CD19 mAb was therefore used for these studies so that the results would be more directly translatable into human studies.

Since a wide variety of results have been obtained using different mouse models to identify the role of B cells during allograft rejection, this study compared the effects of CD20 and CD19 mAb treatment in four distinct allograft rejection models: fully mismatched acute cardiac, chronic renal, and acute skin allografts, and minor-Ag mismatched skin allografts. Using these model systems, B cells and allograft-specific Ab were found to be required for the pathogenesis of chronic kidney allograft rejection, since only CD19 mAb prevented rejection in this model. By contrast, B cells (B10 cells) can exert inhibitory functions during skin allograft rejection because B cell depletion enhanced allograft-specific cellular immune responses and rejection. Thereby, B cells can either positively or negatively regulate allograft rejection depending on the nature of the allograft and the intensity of the rejection response.

Materials and Methods

Mice, Abs, and immunotherapy

Hemizygous huCD19Tg (TG-1 line) mice were as described (26, 30). C57BL/6, DBA/2, 129/X1, B6.PL Thy1^a/Cy (B6.Thy1.1$^+$), C57BL/6-Tg(TcraTcrb)425Cbn/JB6 (OT-II), and C57BL/6-Tg(TcraTcrb)1100Mjb/J (OT-I) mice were from The Jackson Laboratory (Bar Harbor, ME). OT-II and OT-I transgenic mice generate CD4$^+$ and CD8$^+$ T cells that respond to peptides 323–339 and 257–264 of OVA, respectively (31, 32). OT-II and OT-I mice (Thy1.2$^+$) were crossed to B6.Thy1.1$^+$ mice to generate Thy1.1-expressing T cells for adoptive transfer experiments. In some experiments, mice received drinking water containing BrdU (1 mg/ml; Sigma-Aldrich, St. Louis, MO). Mice were housed in a specific pathogen-free barrier facility and used at 6–12 weeks of age. To induce B cell depletion *in vivo*, sterile and endotoxin-free CD20 (MB20-11), CD19 (FMC-63, ref. 33), or isotype-matched control mAb (250 μg) in 200 μl PBS were injected through lateral tail veins as described (21, 22). The Duke University Animal Care and Use Committee approved all studies.

Mouse CD20 mAb (MB20-11, ref. 34) was conjugated to Alexa 488 according to the manufacturer's directions (Invitrogen). FITC-, PE-, PE-Cy5-, APC, PE-Cy7, or biotin-conjugated mouse Thy1.1 (OX-7), CD4 (H129.19), CD8 (53–6.7), B220 (RA3–6B2), CD1d (1B1), CD21 (7G6), CD24 (M1/69), CD138 (281-2), and human CD19 (HIB19) mAbs were from Becton Dickinson (BD; San Jose, CA). Fluorescently-conjugated goat anti-mouse IgG and IgM polyclonal Abs were from Southern Biotech (Birmingham, AL). Rat anti-mouse C4d mAb, rat anti-mouse IgM mAb, and HRP-conjugated goat anti-Rat IgG polyclonal Ab were from Santa Cruz Biotechnology (Santa Cruz, CA). HRP-conjugated anti-mouse IgG was from Vector Laboratories (Burlingame, CA).

Cell preparation and immunofluorescence analysis

Single-cell leukocyte suspensions from BM, spleen, and peripheral LN (axillary, brachial, and inguinal) were generated by gentle dissection, and erythrocytes were hypotonically lysed. For multi-color immunofluorescence analysis, single cell suspensions (10^6 cells) were stained at 4°C using predetermined optimal concentrations of mAb for 25 min, as described (26). Cells with the forward and side light scatter properties of lymphocytes were analyzed using either a FACScan or LSR-II flow cytometer (BD). Background staining was assessed using non-reactive, isotype-matched control mAbs (Caltag Laboratories, San Francisco, CA). Intracellular BrdU staining was performed using the BrdU Flow kit (BD) according to the manufacturer's instructions.

ELISAs

Serum Ig concentrations were determined by ELISA as described (30). Serum autoAb levels against ssDNA and histone were determined by ELISA using boiled calf thymus DNA (Sigma– Aldrich) or histone-coated microtiter plates (Sigma–Aldrich), respectively, as described (27).

ELISPOT Assays

Single cell BM and spleen suspensions were added to Immobilon-P Multiscreen 96-well plates (Millipore, Billerica, MA) that were pre-coated with polyclonal anti-mouse Ig (H+L) Ab (5 μg/ml; Southern Biotech) at either 10^4, 10^5, or 10^6 cells per well in culture medium (100 μl; RPMI 1640 containing 10% FCS, 10 mM glutamine, 100 U/ml penicillin/streptomycin, and 55 μM β-mercaptoethanol). After incubating the plates for 3 h at 37°C in a humidified CO_2 incubator, the plates were washed 3 times and incubated with alkaline phosphatase-conjugated polyclonal goat anti-mouse IgM or IgG Abs (Southern Biotech) for

1 h at room temperature. After washing, the plates were developed using BCIP/NBT substrate (Sigma-Aldrich).

Mouse cardiac transplantation

Heterotopic murine cardiac transplants were as described (35). Recipient C57BL/6–129 (H-2b) mice were anesthetized using isoflurane and prepared by separating the vena cava and aorta between the renal vasculature and the iliac bifurcation. The donor heart was dissected from a fully MHC-mismatched (DBA/2; H-2d) mouse, and an end-to-side anastomosis was created between the recipient aorta and the donor heart ascending aorta. A similar vascular anastomosis was created between the donor superior vena cava and the inferior vena cava of the recipient. The total ischemic time averaged 15 min and was not different between the groups. Surgical mortality of the recipients was less than 10%. Allograft survival was determined by directly palpating the cardiac impulse through the abdominal wall, with graft failure defined as the cessation of a palpable heartbeat.

Measurement of allograft-specific Ab production

Serum Ab generated in response to allografting was evaluated using cell lines and indirect immunofluorescence staining assays. The P815 cell line was purchased from ATCC (Manassas, VA) and was cultured in DMEM medium containing 10% FCS, 200 mg/ml penicillin, 200 U/ml streptomycin, 4 mM L-Glutamine, and 50 mM β-mercaptoethanol (all from Invitrogen, Carlsbad, CA). The AG8 cell line (ATCC) was cultured in RPMI 1640 media containing the same supplements used for culturing P815 cells. Sera from mice were diluted (1:40) and incubated with P815 cells (for DBA/2 mice) or AG8 cells (for BALB/C mice) for 30 min at 4°C. The cells were then washed three times, incubated with fluorochrome-conjugated secondary polyclonal anti-mouse IgG or IgM Abs, and analyzed by flow cytometry on a FACScan flow cytometer (BD). Staining obtained using secondary Ab alone was considered background, with these MFI values (<10) subtracted from the experimental values.

Skin grafting

The skin graft procedures were modified from the methods of Billingham (36). Briefly, dorsal skin was dissected from donor mice after removal of hair with electric clippers and cleansing with 70% ethanol. Subcutaneous fascia was gently removed from the undersurface of donor skin with a Number 15 scalpel. The prepared donor skin was then stored at 4°C on PBS-soaked gauze in sterile petri dishes until use (generally within 90 min). Recipient mice were anesthetized with pentobarbital administered i.p. at a dose of 0.7 mg/g body weight. Hair was removed from the dorsolateral skin of recipient mice, and skin was cleansed with 70% ethanol and painted with flexible collodian. Eight-millimeter-diameter graft beds were prepared by removing the epidermis and superficial dermis leaving the fascia layer intact. Skin grafts were then placed by trimming donor skin to the graft beds. Grafts were dressed with petroleum-coated Telfa gauze held in place with circumferential bandages. Dressings were removed on day 6 after graft placement. Mice were monitored daily following surgery. Duplicate grafts were placed on each mouse, and syngeneic skin grafts served as controls for non-specific inflammation related to surgery. Grafts were considered to be rejected at the time of sloughing or upon complete conversion to a hard avascular eschar.

Adoptive transfer experiments

Donor Thy1.1$^+$ OT-II or OT-I T cells from pooled spleens and LN were enriched using CD4$^+$ and CD8$^+$ T cell isolation kits (Miltenyi Biotec), respectively, and labeled with CFSE Vybrant™ CFDA SE fluorescent dye (1 mM; Invitrogen-Molecular Probes, Carlsbad, CA) according to the manufacturer's instructions. Labeled Thy1.1$^+$ cells (2.5×10^6) were given

i.v. to Thy1.2$^+$ congenic recipients 1 d before skin grafting. The proliferation of transferred cells was visualized by flow cytometry analysis of CFSE-labeled Thy1.1$^+$ cells. Transferred OT-II CD4$^+$ or OT-I CD8$^+$ T cells were identified by Thy1.1 and CD4 or CD8 mAb staining, respectively.

Kidney Transplantation

Vascularized kidney transplants were as described (37). Mice were anesthetized with isoflurane, and the donor kidney, ureter, and bladder were harvested en bloc, including the renal artery with a small aortic cuff and the renal vein with a small vena caval cuff. These vascular cuffs were anastomosed to the recipient abdominal aorta and vena cava, respectively, below the level of the native renal vessels. Donor and recipient bladders were attached dome to dome. The right native kidney was removed during transplant, and the left native kidney was removed through a flank incision 1–3 d later. The adrenal glands and their blood supply were preserved intact. Mice surviving 100 d were sacrificed with 100 d survival used when calculating mean survival times. These mice were considered to be survivors in the Log-Rank statistical analysis.

Kidney histopathologic and immunohistology studies

A portion of the transplanted kidneys was placed in buffered 10% formalin, sectioned, and stained with H&E, PAS, and Masson's Trichrome. All tissues were examined by a pathologist (P.R.) masked to the experimental groups. The overall severity of rejection was determined by the pattern and intensity of inflammatory cell infiltrates in both glomeruli and tubulointerstitial areas, and glomerular, tubular, and vascular abnormalities. Grading was performed using a semiquantitative scale in which 0 represented the absence of histologic abnormalities, and 1+, 2+, 3+, and 4+ represented mild, moderate, moderately severe, and severe abnormalities, respectively, as described (38, 39). An overall histologic score was obtained for each kidney by summing the individual grades for the glomeruli, tubules, interstitium, and vasculature (39).

To assess C4d, IgG, and IgM deposition, a portion of transplanted kidneys was removed, embedded in OCT compound, and snap frozen in pre-cooled 2-methylbutane. Tissue sections (5 μm) were cut with a cryostat, air dried, fixed in acetone, washed with PBS (pH 7.4), blocked with normal goat serum, and stained with the appropriately diluted primary mAb. Primary Ab binding was detected with a species-specific HRP-conjugated secondary Ab followed by development using 3,3' Diaminobenzidine as the substrate (Vector Laboratories). Grading of the C4d, IgG, and IgM staining intensities of peritubular capillaries was performed independently by blinded pathologists (C.M. and S.V.S.) using a semiquantitative scale, in which 0 represented no staining, and 1+, 2+, and 3+ represented mild, moderate, and severe staining, respectively.

Statistical analysis

All data are shown as means ± SEM. Significant differences between sample means were determined using the Student's t test. Significance in survival studies was determined using the Log-Rank test.

Results

CD20 and CD19 mAbs effectively deplete different B cell populations

Mouse anti-mouse CD20 (MB20-11) and mouse anti-human CD19 (FMC63) mAbs deplete B cells in C57BL/6 mice and C57BL/6 huCD19Tg mice, respectively (21, 22). However, C57BL/6–129 (F1) huCD19Tg mice were utilized for cardiac and renal allografts in the current studies since their larger size and hybrid vigor enhanced survival during and after

allograft surgery. Therefore, B cell depletion with these CD20 and CD19 mAbs was also compared side-by-side in C57BL/6–129 huCD19Tg mice given isotype control, CD20, or CD19 mAb for 7 d.

Within the BM, CD19 mAb treatment decreased $B220^+$ B cell numbers by 90% (p=0.003), while CD20 mAb treatment had a small effect (Figure 1A). Both CD20 and CD19 mAb treatments decreased IgM^+B220^{hi} mature B cell numbers by >97% (p=0.003). CD19 mAb treatment also depleted IgM^+B220^{low} immature B cells by >98% (p=0.03) and $IgM^-B220^{low}CD43^-$ pre-B cells by 94% (p=0.02; Table I). In the periphery, CD20 or CD19 mAb treatment reduced blood $B220^+$ cell numbers by >97% (p=0.001), spleen $B220^+$ cell numbers by >78% (p≤0.009), and LN $B220^+$ cell numbers by >83% (p≤0.005) (Figure 1B–D). In the spleen, CD20 mAb treatment depleted 59% (p=0.02) of transitional-1, 85% (p=0.001) of transitional-2, and 91% (p=0.003) of marginal zone B cells. CD19 mAb depleted 77% (p=0.002) of transitional-1, 81% (p=0.002) of transitional-2, and 72% (p=0.008) of marginal zone B cells. Thus, CD20 and CD19 mAb treatment depleted peripheral B cells similarly, while CD19 mAb depleted pre-B and immature BM B cells in huCD19Tg mice.

CD19 mAb, but not CD20 mAb treatment depletes serum IgG in naïve mice

CD20 mAb treatment does not alter serum Ig levels in C57BL/6 mice (25), while CD19 mAb treatment depletes serum IgM, IgG, and autoantibodies (autoAbs) in C57BL/6 huCD19Tg mice (22). To directly compare the effects of CD20 and CD19 mAbs on serum Ig levels in the same mouse line, C57BL/6 huCD19Tg mice were treated with control, CD20, or CD19 mAb, with serum harvested over a 6 mo time period. Serum Ig levels increase in huCD19Tg mice due to enhanced CD19 signaling, with these mice producing autoAbs and becoming hypergammaglobulinemic with age (30). After 1 mo of CD20 or CD19 mAb treatment, serum IgM levels decreased by 83% and 75%, respectively (p<0.00001), relative to their levels before mAb administration (Figure 2A). After 1 mo of CD19 mAb treatment, serum IgG levels decreased by 78% (p<0.00001), while CD20 mAb treatment only prevented the increase in IgG levels observed in control mAb-treated mice (Figure 2B, p=0.02 relative to control mAb). Serum Ig levels in mAb-treated mice began to increase after 2 mo, when B cells returned to the periphery (21, 24).

The effect of CD20 and CD19 mAb treatments on IgG autoAb levels was also determined in huCD19Tg mice. After 1 mo of CD19 mAb treatment, anti-ssDNA and anti-histone IgG autoAb levels were reduced by 75% (p=0.0002) and 57% (p<0.0001), respectively, while these IgG autoAbs were maintained in CD20 mAb-treated mice (Figure 2C–D). Thus, CD19 mAb treatment significantly reduced normal and auto-reactive serum IgG levels, while CD20 mAb treatment only delayed age-associated increases in Ab and autoAb production.

CD19 mAb treatment depletes Ab-secreting plasma cells

Because CD19 mAb treatment reduced serum IgG levels while CD20 mAb did not, the effect of CD20 and CD19 mAb treatment on plasma cell numbers was assessed. Plasmablasts and plasma cells express CD138, a cell surface marker used for Ab-secreting cell (ASC) identification (40, 41). Short-lived plasmablasts ($CD138^{hi}BrdU^+$) and long-lived plasma cells ($CD138^{hi}BrdU^-$) can be phenotypically identified using CD138 staining in combination with *in vivo* BrdU labeling (42). Therefore, huCD19Tg mice were fed BrdU for 10 d before treatment with CD19, CD20, or control mAbs, with spleen and BM cells assessed for CD138 and BrdU staining 7 d later. CD19 mAb treatment depleted 80% and 58% (p≤0.0009) of BM $CD138^{hi}BrdU^+$ and $CD138^{hi}BrdU^-$ cells, respectively (Figure 3A). CD20 mAb treatment only depleted 33% (p=0.04) of BM $CD138^{hi}BrdU^+$ plasmablasts, with no significant effect on $CD138^{hi}BrdU^-$ plasma cells. Spleen $CD138^{hi}BrdU^+$ and

$CD138^{hi}BrdU^{-}$ cells were decreased by 89% (p=0.02) and 79% (p=0.002), respectively, following CD19 mAb treatment. CD20 mAb treatment depleted splenic $CD138^{hi}BrdU^{+}$ plasmablasts and $CD138^{hi}BrdU^{-}$ plasma cells by 37% (not significant) and 54% (p=0.02), respectively. Therefore, CD20 mAb treatment had limited effects on long-lived BM or splenic plasma cells, while CD19 mAb treatment depleted the majority of both short-lived plasmablasts and long-lived plasma cells in the BM and spleen.

The effect of mAb treatment on IgM and IgG ASC numbers was assessed directly in huCD19Tg mice 7 d after treatment with control, CD20, or CD19 mAb. In the BM, CD19 mAb treatment decreased IgM ASC numbers by 69% (p=0.03) and IgG ASC numbers by 66% (p=0.002) (Figure 3B). Splenic IgM and IgG ASC numbers were reduced by 63% and 68% ($p \leq 0.005$), respectively. B contrast, CD20 mAb treatment had no effect on ASC numbers in either tissue. Thus, only CD19 mAb treatment depleted both IgM and IgG ASCs.

Cell surface CD20 is downregulated during plasma cell differentiation in humans and mice (25, 43). Mouse CD19 expression is lost in a similar manner on mouse plasma cells (data not shown), while human CD19 loss occurs later during human plasma cell development (29). Whether CD20 and CD19 mAbs differentially deplete mouse plasmablasts due to prolonged cell surface molecule expression on $B220^{+}CD138^{hi}$ plasmablasts or more differentiated $B220^{lo}CD138^{hi}$ plasmablasts in the spleen and BM of huCD19Tg mice was assessed (Figure 3C). Compared to splenic $B220^{+}CD138^{-}$ follicular B cells, CD20 expression was decreased by 50% on splenic $B220^{lo}CD138^{hi}$ plasmablasts ($p<0.00001$) and by 62% on BM $B220^{lo}CD138^{hi}$ plasmablasts ($p<0.00001$). By contrast, CD19 expression was increased by 2.7-fold and 2.2-fold ($p<0.0001$), respectively, on splenic and BM $B220^{+}CD138^{hi}$ plasmablasts when compared to splenic follicular B cells. CD19 expression subsequently decreased so that spleen $B220^{low}CD138^{hi}$ plasmablasts and follicular B cells expressed similar CD19 densities, while BM $B220^{low}CD138^{+}$ plasmablast densities ranged between 70–100%. Thus, while CD20 levels decreased during plasma cell differentiation, CD19 expression remained high on plasmablasts.

CD19 mAb treatment inhibits graft-specific IgG generation during cardiac allograft rejection

The contributions of B cells and plasma cells to solid organ allograft rejection were assessed in an acute cardiac allograft model where C57BL/6–129 mice normally reject fully MHC-mismatched hearts from BALB/C-DBA/2 (F1) mice within 7–9 d (44). huCD19Tg mice were treated with control, CD20, or CD19 mAb 7 d before the mice received heterotopic DBA/2 cardiac allografts, with graft survival monitored daily. Grafts in all mice were rejected within 7 to 9 d, with no significant differences between groups (control mAb, 7.8±0.2 d; CD20 mAb, 8±0.6 d; CD19 mAb, 6.8±0.3 d; Figure 4A). However, CD19 mAb treatment inhibited the generation of serum allograft-specific IgM and IgG Abs that were reactive with the DBA/2-derived P815 cell line (Figure 4B). B cell depletion with CD20 and CD19 mAbs decreased serum allograft-specific IgM levels by 56% and 71%, respectively ($p \leq 0.006$). CD19 mAb treatment decreased serum allograft-specific IgG levels by 83% (p=0.004), while CD20 mAb treatment had no effect. Thus, CD19 mAb treatment did not affect acute cardiac allograft rejection, but significantly reduced the quantity of allograft-specific IgG in serum.

CD20 mAb treatment impairs skin allograft-specific IgG generation

Since CD20 mAb treatment did not affect acute rejection of a directly vascularized organ allograft, its effects on fully MHC-mismatched tissue allograft rejection were assessed. huCD19Tg mice contain significantly higher numbers of regulatory B10 cells that function to suppress contact hypersensitivity and immune responses initiated in the skin (8).

Therefore, wild type C57BL/6 mice and CD20 mAb were used for the skin grafting experiments to exclude the immunosuppressive effects of increased B10 cell numbers in huCD19Tg mice. Because of this, the effect of CD19 mAb treatment on skin allograft rejection was not assessed. Wild type C57BL/6 mice were treated with control or CD20 mAb 7 d before receiving fully MHC-mismatched full-thickness BALB/C skin grafts. Grafts were rejected in both the control and CD20 mAb-treated groups, with mean survival times of 11.0±0.2 and 10.7±0.2 d, respectively (Figure 5A). However, serum BALB/C-specific IgM levels were reduced by 68% (p=0.02) in CD20 mAb-treated mice 14 d after skin grafting (21 d after mAb injection) in comparison with control mAb-treated mice, and graft-specific IgG levels were decreased by 75% (p=0.005) (Figure 5B). Thus, mature B cell depletion had no effect on acute skin allograft rejection, but did inhibit the generation of serum allograft-specific IgG.

CD20 mAb treatment accelerates minor Ag-mismatched skin allograft rejection

The effect of mature $CD20^+$ B cell depletion on the rejection of skin allografts expressing a single, defined Ag was assessed to reveal differences in rejection that may not have been seen in the context of the vigorous rejection of fully MHC-mismatched grafts. C57BL/6 mice were treated with control or CD20 mAb 7 d before receiving skin grafts from C57BL/6 transgenic act-mOVA mice that express cell surface-bound OVA protein (45). CD20 mAb-treated mice rejected act-mOVA grafts significantly faster (mean 14.7 ± 0.7 d) than mice that received control mAb (17 ± 0.7 d; p=0.019, log rank test; chi square=5.5, df=1; Figure 5C). OVA-specific IgM or IgG responses were not detected in either CD20 or control mAb-treated mice 21 d after grafting (data not shown), reflecting the weak Ab responses generally observed for minor histocompatibility Ags (46). Thus, mature B cell depletion accelerated the rejection of Ag-mismatched skin grafts.

The effects of CD20 mAb treatment on T cell function were assessed since C57BL/6 mice effectively reject act-mOVA skin grafts in a T cell-dependent manner (45). C57BL/6 mice were given either control or CD20 mAb 6 d before being given CFSE-labeled $Thy1.1^+$ $CD4^+$ or $CD8^+$ T cells from OVA peptide-specific OT-II or OT-I transgenic mice, respectively (31, 32). One d later, all mice received act-mOVA skin grafts. The spleen and peripheral LN draining the site of the skin graft were isolated 5 d later, with CFSE dilution by $Thy1.1^+$ $CD4^+$ or $CD8^+$ T cells analyzed by flow cytometry to quantify T cell proliferation. Draining LN $Thy1.1^+CD4^+$ OT-II cells from CD20 mAb-treated mice diluted CFSE two-fold greater (p=0.006) than control mAb-treated mice (Figure 5D), while splenic OT-II cells from CD20 mAb-treated mice diluted CFSE 1.7-fold greater than control mice (Figure 5E). By contrast, $CD8^+$ OT-I cells proliferated similarly in the LN and spleen of both control and CD20 mAb-treated mice receiving act-mOVA skin grafts (data not shown). Thus, B cell depletion enhanced $CD4^+$ T cell activation and proliferation in response to Ag-mismatched tissue transplants, which paralleled accelerated graft rejection.

CD19 mAb treatment prevents chronic renal allograft rejection

A renal allograft model was used to assess the contributions of B cells and plasma cells to chronic allograft rejection (47). huCD19Tg mice were treated with control, CD20, or CD19 mAb 7 d before being transplanted with a kidney from a fully MHC-mismatched DBA/2 donor. After a bilateral native nephrectomy, graft rejection was determined by assessing mouse survival. Kidney allografts in mice survive for prolonged periods without immunosuppression, but develop pathological features consistent with chronic allograft rejection in humans. Graft survival was similar in control and CD20 mAb-treated mice (mean survival time for control mAb, 54±8 d; CD20 mAb, 53±9 d), with only 20–22% of mice surviving >100 d (Figure 6A). However, CD19 mAb treatment significantly enhanced survival (84±9 d) when compared to control (p=0.023, log rank test; chi square=5.2, df=1)

or CD20 (p=0.035, log rank test; chi square=4.4, df=1) mAb-treated mice, with 67% of CD19 mAb-treated mice surviving for >100 d.

Whether CD20 or CD19 mAb treatment affected the development of IgM and IgG allograft-specific Ab responses was assessed in separate groups of allografted mice by harvesting serum 21 d after kidney grafting. Pre-treatment with both CD20 and CD19 mAbs decreased serum allograft-specific IgM levels by 57% and 77%, respectively ($p \leq 0.002$; Figure 6B). Allograft-specific IgG levels were decreased to background levels in CD19 mAb-treated mice (p=0.005) and decreased by 67% (p=0.02) with CD20 mAb treatment (Figure 6B). Thus, CD19 mAb treatment abrogated the generation of quantifiable serum allograft-specific IgG responses while CD20 mAb only inhibited serum allograft-specific IgG responses.

The severity of renal morphologic abnormalities was assessed 21 d after transplantation by H&E, PAS, and Masson's Trichrome staining to determine whether enhanced allograft survival in CD19 mAb-treated mice was associated with reduced kidney pathology. In control mAb-treated allografts, the predominant finding was the intense infiltration of inflammatory cells within interstitial regions of the kidney (Table II), which was less severe in CD20 (32% decrease, p=0.004) and CD19 (43%, p=0.0006) mAb-treated mice (Figure 7A, data not shown). Tubular pathologic changes (tubulitis, the defining feature of acute renal allograft rejection) were most severe in control mice, but were decreased (39% decrease, p=0.01) in CD20 mAb-treated mice. However, there was a 70% decrease (p=0.001) in tubular pathology in CD19 mAb-treated mice when compared with control mice. Tubular pathology was also decreased by 51% in CD19 mAb-treated mice when compared to mice receiving CD20 mAb (p=0.04; Table II). In general, glomerular pathologic changes were variable and less pronounced. An overall histologic score for each kidney was obtained by summing the individual grades for the glomeruli, tubules, interstitium, and vasculature pathologies (Figure 7A, Table II). Kidneys from control mAb-treated mice showed the highest overall pathologic score, while the mean scores for kidneys from CD20 or CD19 mAb-treated mice were decreased by 33% (p=0.03) and 47% (p=0.006), respectively, when compared to control mice.

Complement fragment C4d deposition in peritubular capillaries is a hallmark of Ab-mediated kidney allograft rejection and is closely associated with chronic rejection in renal transplant patients (48). Therefore, C4d deposition was assessed by immunohistochemistry in the allografted kidneys of mAb-treated mice 3 wks after transplant surgery. Virtually all of the capillaries in mice receiving control or CD20 mAb exhibited an intense homogenous pattern of mural C4d staining, while most of the CD19 mAb-treated mice showed only weak homogeneous deposition of C4d within the capillary walls (Figure 7B). The mean intensity of C4d deposition was decreased by 30% ($p \leq 0.008$) in the peritubular capillaries of mice receiving CD19 mAb when compared to control or CD20 mAb-treated mice. Similarly, intense homogenous IgG staining was seen within most of the peritubular capillary walls of kidneys from control or CD20 mAb-treated mice, while only occasional capillaries in CD19 mAb-treated mice showed weak mural IgG staining (Figure 7D). The mean intensity of capillary IgG deposition was decreased by 24%, ($p \leq 0.02$) in both CD20 and CD19 mAb-treated mice when compared with control mice. Intense intraluminal and mural IgM staining of peritubular capillaries was also seen in kidneys from control mAb-treated mice, while weak to moderately intense staining of many peritubular capillary walls was seen in kidneys from mice receiving CD20 mAb (Figure 7C). Most of the vessels in kidneys from CD19 mAb-treated mice were devoid of IgM staining and only weak focal staining of rare peritubular capillaries was seen. The intensity of IgM staining was decreased by 33% (p=0.004; Figure 7C) in both CD20 and CD19 mAb-treated mice when compared with control mice. Thus, CD19 mAb treatment inhibited C4d, IgG, and IgM deposition in allografted kidneys.

CD19 mAb treatment depletes pre-existing allograft-specific IgG

Because CD19 mAb treatment depleted serum IgG levels in naïve mice and prevented the generation of serum allograft-specific IgG in mice receiving heart and kidney allografts, whether CD19 mAb could deplete pre-existing allograft-specific IgG levels was determined. huCD19Tg mice were immunized and boosted i.p. with 10^7 DBA/2 splenocytes at weeks 0 and 2. Three weeks after the boost (at the peak of the Ab response), the mice received control, CD20, or CD19 mAb. Serum DBA/2-specific IgG was assessed using indirect immunofluorescence staining with flow cytometry analysis. All mice in each of the three groups mounted similar allograft-specific IgG responses. At 10 weeks post-mAb treatments, CD19 mAb treatment reduced allograft-specific IgG levels by 59% compared to control mice ($p=0.008$), while CD20 mAb had no effect (Figure 6C). Thus, CD19 mAb treatment not only inhibited the induction of allograft-specific IgG in naïve mice, but reduced the quantity of allograft-specific IgG in the serum of allo-sensitized mice.

Discussion

B cell depletion by highly effective CD20 and CD19 mAbs in side-by-side comparisons confirmed that CD19 mAb depletes a broader spectrum of B cells in huCD19Tg mice than CD20 mAb due to CD19 being expressed both early and late during B cell development (Figures 1 and 3). As a consequence, chronic kidney allograft rejection was significantly inhibited by CD19, but not CD20 mAb treatment (Figure 6). Furthermore, CD19 mAb treatment inhibited the production of serum allograft-specific IgG during acute cardiac and chronic renal allograft rejection and reduced serum IgG and pre-existing levels of serum allograft-specific Ab, while CD20 mAb did not (Figures 4–6). These differences are explained by the finding that CD20 mAb depleted mature B cells, while CD19 mAb depleted both mature B cells and a significant fraction of plasmablasts and Ab-secreting plasma cells (Figures 1–3). Thereby, it is likely that allograft-specific Ab production in combination with B cell Ag presentation and/or costimulation contributes to chronic renal allograft rejection. Thus, CD19 mAb depletion of mature B cells and a significant portion of the plasmablast and Ab-secreting B cell pool may be advantageous for treating sensitized transplant recipients with pre-existing allograft-specific Abs and transplant patients undergoing Ab-mediated acute or chronic rejection when compared with CD20 mAb.

While B cells contributed to chronic renal allograft rejection, B cell depletion accelerated skin graft rejection. Specifically, skin grafts expressing a single foreign Ag were rejected significantly faster following mature B cell depletion by CD20 mAb (Figure 5C). The proliferation of alloantigen-specific $CD4^+$ T cells in grafted mice was also significantly enhanced by B cell depletion (Figure 5D–E). Since CD20 mAb treatment only depletes B cells (3), these results demonstrate that some B cells normally function to inhibit allograft destruction. Most likely, CD20 mAb depletion of regulatory IL-10-competent B10 cells (7, 49) explains the hastened graft rejection and augmented alloantigen-specific $CD4^+$ T cell response observed in this allograft model. Similarly, B10 cell depletion by CD20 mAb treatment exacerbates contact hypersensitivity responses and the onset and severity of EAE (8, 9). Enhanced skin graft rejection in the absence of B cells has also been suggested previously; BALB/B skin may be rejected faster in μMT mice than in wild type C57BL/6 mice (46), and act-mOVA skin grafts were rejected faster in four μMT mice (45). In a previous study, B cell depletion using a different CD20 mAb before grafting skin with a single MHC difference did not affect rejection, although all skin grafts were acutely rejected within 10 d in that model (50). Similarly, B cell depletion did not alter the acute rejection of MHC-mismatched skin grafts in the current study (Figure 5A). Thereby, since B cells do not act as APCs during skin graft rejection (14), the negative regulatory activities of B cells are likely to be most easily observed when alloantigen concentrations are low and the Ab contributions of B cells to pathology are reduced. Thus, B cells can negatively regulate

allograft rejection depending on the nature of the allograft and the intensity of the rejection response. It is important to note that while B cells suppressed rejection in one model and promoted rejection in another, the opposing activation and inhibitory capacities of B cells are likely to occur simultaneously during most immune responses, with the overall balance between activation and inhibition being more obvious in some cases/diseases, such as during accelerated rejection of minor-mismatched skin grafts.

B cell contributions to acute cardiac rejection, chronic renal rejection, and skin graft rejection also depended on the nature of the allograft and the intensity of the rejection response. B cell depletion did not affect acute cardiac allograft survival (Figure 4) or alter the rejection of fully MHC disparate BALB/C skin grafted onto C57BL/6 mice (Figure 5A). Similarly, mature B cell depletion by CD20 mAb did not affect chronic renal rejection (Figure 6). These findings are consistent with studies where μMT and wild type C57BL/6 mice rejected BALB/C hearts (11), C3H hearts (12), or C3H aortic segments (13) similarly. Xenotransplants are also rejected normally in *Xid* mice (51), and BALB/C skin is rejected normally in agammaglobulinemic B10.BR mice treated chronically with anti-IgM serum to deplete B cells (52). Reduced allograft-specific Ab quantities following B cell depletion did not appear to affect skin graft (Figure 5A–B) or cardiac allograft (Figure 4) rejection, even though the addition of exogenous allograft-specific Ab is capable of inducing skin graft destruction (53, 54). Further, allograft-specific Abs can cause pathological lesions in mouse cardiac allografts (55) and allograft rejection in immunosuppressed mice (11, 15, 16). B cells can also function as APCs during acute rejection (14). However, when Ag is present at high levels in B cell-depleted mice, dendritic cells and/or macrophages appear sufficient for Ag presentation (3). Thereby, B cell depletion may only prolong allograft survival when carried out in conjunction with the suppression of T cell responses (11, 56, 57) since vascularized grafts can represent an enormous alloantigen pool that drives T cell activation. Consistent with this, CD20 mAb pretreatment abrogates cellular and humoral immune responses to minor Ag-mismatched skin allograft rejection (Figure 5D), and to model Ags and in autoimmune disease where the Ag doses are far lower than found in fully vascularized organ allografts (3, 25). Thus, mature B cell depletion with CD20 or CD19 mAb may optimally prolong graft survival only when the alloantigen load is reduced or when additional immunosuppressive agents are used to inhibit T cell activation.

The current CD20 mAb results in mouse allograft models mimic what has been observed in the clinic when treating allograft rejection with the CD20 mAb Rituximab. Because Rituximab treatment has poor and variable effects on preformed allograft-specific Ab levels in patients (58), it is often combined with plasmapheresis, intravenous Ig, splenectomy, and/or other immunosuppressive drugs to desensitize patients before grafting (59) or to prevent Ab-mediated rejection (60). For example, using a combination of Rituximab and intravenous Ig for desensitization, 80% of patients could be transplanted, with 94% of grafts surviving at 1 yr (61). Combining plasmapheresis, low dose intravenous Ig, and Rituximab treatment has also successfully decreased existing allograft-specific Ab titers in some patients (62). In eight patients undergoing cardiac transplant rejection, humoral rejection was reversed when Rituximab was used as a first-line therapy in association with cyclosporine, prednisone, and mycophenolate (63). In another study, Rituximab, in combination with steroids, plasmapheresis, and/or anti-thymocyte globulin successfully treated biopsy-confirmed kidney rejection (64). Although the specific contribution of CD20 mAb treatment is clouded in these patients by the presence of other immunosuppressive therapies, the current comparative results obtained using CD19 mAb in side-by-side models of rejection argue that CD19 mAb may be even more effective than CD20 mAb for desensitization and the treatment of acute and chronic Ab-mediated rejection.

This study demonstrates that B cells can either positively or negatively regulate graft rejection depending on the nature of the allograft and the intensity of the rejection response. Inhibitory roles for regulatory B cells (B10 cells) during organ rejection may be commonly obscured by the strength of immune responses against mismatched tissue and organ grafts. Nonetheless, the potential for human B cell negative regulatory function during allograft rejection is suggested by a recent suspended clinical trial where patients receiving Rituximab suffered acute cellular rejection of kidney grafts at a greater rate (65). These and previous studies also indicate that mature B cell depletion alone with CD20 mAb will not be sufficient to prevent or treat solid organ allograft rejection due to the dominant and overlapping functions of T cells and other effector cells. Thereby, CD19 mAb may offer a new approach for depleting both B cells and some plasma cells to impair Ag presentation, reduce preexisting allograft-specific Ab levels, and inhibit the generation of new allograft-specific Abs. Thus, the current results emphasize that B cells contribute in multiple ways to rejection, and demonstrate the balance that exists between the positive and negative regulatory functions of B cells during allograft rejection.

Acknowledgments

We thank Dr. Heddy Zola for providing the FMC63 mAb used in these studies.

Nonstandard Abbreviations Used

huCD19Tg	human CD19 transgenic
autoAb	autoantibody
ASC	Ab-secreting cell

References

1. Linton PJ, Harbertson J, Bradley LM. A critical role for B cells in the development of memory CD4 cells. J. Immunol. 2000; 165:5558–5565. [PubMed: 11067910]
2. Crawford A, Macleod M, Schumacher T, Corlett L, Gray D. Primary T cell expansion and differentiation in vivo requires antigen presentation by B cells. J. Immunol. 2006; 176:3498–3506. [PubMed: 16517718]
3. Bouaziz JD, Yanaba K, Venturi GM, Wang Y, Tisch RM, Poe JC, Tedder TF. Therapeutic B cell depletion impairs adaptive and autoreactive $CD4^+$ T cell activation in mice. Proc. Natl. Acad. Sci. USA. 2007; 104:20882–20887.
4. DiLillo DJ, Yanaba K, Tedder TF. B cells are required for optimal $CD4^+$ and $CD8^+$ T cell tumor immunity: therapeutic B cell depletion enhances B16 melanoma growth in mice. J. Immunol. 2010; 184:4006–4016. [PubMed: 20194720]
5. O'Neill SK, Cao Y, Hamel KM, Doodes PD, Hutas G, Finnegan A. Expression of CD80/86 on B cells is essential for autoreactive T cell activation and the development of arthritis. J. Immunol. 2007; 179:5109–5116. [PubMed: 17911596]
6. Linton PJ, Bautista B, Biederman E, Bradley ES, Harbertson J, Kondrack RM, Padrick RC, Bradley LM. Costimulation via OX40L expressed by B cells is sufficient to determine the extent of primary CD4 cell expansion and Th2 cytokine secretion in vivo. J. Exp. Med. 2003; 197:875–883. [PubMed: 12668647]
7. DiLillo DJ, Matsushita T, Tedder TF. B10 cells and regulatory B cells balance immune responses during inflammation, autoimmunity, and cancer. Ann. N. Y. Acad. Sci. 2010; 1183:38–57. [PubMed: 20146707]
8. Yanaba K, Bouaziz J-D, Haas KM, Poe JC, Fujimoto M, Tedder TF. A regulatory B cell subset with a unique $CD1d^{hi}CD5^+$ phenotype controls T cell-dependent inflammatory responses. Immunity. 2008; 28:639–650. [PubMed: 18482568]

9. Matsushita T, Yanaba K, Bouaziz J-D, Fujimoto M, Tedder TF. Regulatory B cells inhibit EAE initiation in mice while other B cells promote disease progression. J. Clin. Invest. 2008; 118:3420–3430. [PubMed: 18802481]
10. Watanabe R, Ishiura N, Nakashima H, Kuwano Y, Okochi H, Tamaki K, Sato S, Tedder TF, Fujimoto M. Regulatory B cells (B10 cells) have a suppressive role in murine lupus: CD19 and B10 cell deficiency exacerbates systemic autoimmunity. J. Immunol. 2010; 184:4801–4809. [PubMed: 20368271]
11. Brandle D, Joergensen J, Zenke G, Burki K, Hof RP. Contribution of donor-specific antibodies to acute allograft rejection: evidence from B cell-deficient mice. Transplantation. 1998; 65:1489–1493. [PubMed: 9645808]
12. Alexander DZ, Pearson TC, Hendrix R, Ritchie SC, Larsen CP. Analysis of effector mechanisms in murine cardiac allograft rejection. Transpl. Immunol. 1996; 4:46–48. [PubMed: 8762009]
13. Gareau A, Hirsch GM, Lee TD, Nashan B. Contribution of B cells and antibody to cardiac allograft vasculopathy. Transplantation. 2009; 88:470–477. [PubMed: 19696629]
14. Noorchashm H, Reed AJ, Rostami SY, Mozaffari R, Zekavat G, Koeberlein B, Caton AJ, Naji A. B cell-mediated antigen presentation is required for the pathogenesis of acute cardiac allograft rejection. J. Immunol. 2006; 177:7715–7722. [PubMed: 17114442]
15. Wasowska BA, Qian Z, Cangello DL, Behrens E, Van Tran K, Layton J, Sanfilippo F, Baldwin WM 3rd. Passive transfer of alloantibodies restores acute cardiac rejection in IgKO mice. Transplantation. 2001; 71:727–736. [PubMed: 11330533]
16. Nozaki T, Amano H, Bickerstaff A, Orosz CG, Novick AC, Tanabe K, Fairchild RL. Antibody-mediated rejection of cardiac allografts in CCR5-deficient recipients. J. Immunol. 2007; 179:5238–5245. [PubMed: 17911609]
17. Joao C, Ogle BM, Gay-Rabinstein C, Platt JL, Cascalho M. B cell-dependent TCR diversification. J. Immunol. 2004; 172:4709–4716. [PubMed: 15067046]
18. Asano MS, Ahmed R. CD8 T cell memory in B cell-deficient mice. J. Exp. Med. 1996; 183:2165–2174. [PubMed: 8642326]
19. Moulin V, Andris F, Thielemans K, Maliszewski C, Urbain J, Moser M. B lymphocytes regulate dendritic cell (DC) function in vivo: increased interleukin 12 production by DCs from B cell-deficient mice results in T helper cell type 1 deviation. J. Exp. Med. 2000; 192:475–482. [PubMed: 10952717]
20. Crowley MT, Reilly CR, Lo D. Influence of lymphocytes on the presence and organization of dendritic cell subsets in the spleen. J. Immunol. 1999; 163:4894–4900. [PubMed: 10528191]
21. Uchida J, Hamaguchi Y, Oliver JA, Ravetch JV, Poe JC, Haas KM, Tedder TF. The innate mononuclear phagocyte network depletes B lymphocytes through Fc receptor-dependent mechanisms during anti-CD20 antibody immunotherapy. J. Exp. Med. 2004; 199:1659–1669. [PubMed: 15210744]
22. Yazawa N, Hamaguchi Y, Poe JC, Tedder TF. Immunotherapy using unconjugated CD19 monoclonal antibodies in animal models for B lymphocyte malignancies and autoimmune disease. Proc. Natl. Acad. Sci. USA. 2005; 102:15178–15183. [PubMed: 16217038]
23. Tedder TF. CD19: a promising B cell target for rheumatoid arthritis. Nat. Rev. Rheumatol. 2009; 5:572–577. [PubMed: 19798033]
24. Hamaguchi Y, Uchida J, Cain DW, Venturi GM, Poe JC, Haas KM, Tedder TF. The peritoneal cavity provides a protective niche for B1 and conventional B lymphocytes during anti-CD20 immunotherapy in mice. J. Immunol. 2005; 174:4389–4399. [PubMed: 15778404]
25. DiLillo DJ, Hamaguchi Y, Ueda Y, Yang K, Uchida J, Haas KM, Kelsoe G, Tedder TF. Maintenance of long-lived plasma cells and serological memory despite mature and memory B cell depletion during CD20 immunotherapy in mice. J. Immunol. 2008; 180:361–371. [PubMed: 18097037]
26. Zhou L-J, Smith HM, Waldschmidt TJ, Schwarting R, Daley J, Tedder TF. Tissue-specific expression of the human CD19 gene in transgenic mice inhibits antigen-independent B lymphocyte development. Mol. Cell. Biol. 1994; 14:3884–3894. [PubMed: 7515149]

27. Sato S, Ono N, Steeber DA, Pisetsky DS, Tedder TF. CD19 regulates B lymphocyte signaling thresholds critical for the development of B-1 lineage cells and autoimmunity. J. Immunol. 1996; 157:4371–4378. [PubMed: 8906812]
28. Sato S, Steeber DA, Jansen PJ, Tedder TF. CD19 expression levels regulate B lymphocyte development: human CD19 restores normal function in mice lacking endogenous CD19. J. Immunol. 1997; 158:4662–4669. [PubMed: 9144478]
29. Nadler LM, Anderson KC, Marti G, Bates M, Park E, Daley JF, Schlossman SF. B4, a human B lymphocyte-associated antigen expressed on normal, mitogen activated, and malignant B lymphocytes. J. Immunol. 1983; 131:244–250. [PubMed: 6408173]
30. Engel P, Zhou L-J, Ord DC, Sato S, Koller B, Tedder TF. Abnormal B lymphocyte development, activation and differentiation in mice that lack or overexpress the CD19 signal transduction molecule. Immunity. 1995; 3:39–50. [PubMed: 7542548]
31. Barnden MJ, Allison J, Heath WR, Carbone FR. Defective TCR expression in transgenic mice constructed using cDNA-based α- and β-chain genes under the control of heterologous regulatory elements. Immunol. Cell. Biol. 1998; 76:34–40. [PubMed: 9553774]
32. Hogquist KA, Jameson SC, Heath WR, Howard JL, Bevan MJ, Carbone FR. T cell receptor antagonist peptides induce positive selection. Cell. 1994; 76:17–27. [PubMed: 8287475]
33. Zola H, MacArdle PJ, Bradford T, Weedon H, Yasui H, Kurosawa Y. Preparation and characterization of a chimeric CD19 monoclonal antibody. Immunol. Cell Biol. 1991; 69:411–422. [PubMed: 1725979]
34. Uchida J, Lee Y, Hasegawa M, Liang Y, Bradney A, Oliver JA, Bowen K, Steeber DA, Haas KM, Poe JC, Tedder TF. Mouse CD20 expression and function. Int. Immunol. 2004; 16:119–129. [PubMed: 14688067]
35. Mannon RB, Kotzin BL, Nataraj C, Ferri K, Roper E, Kurlander RJ, Coffman TM. Downregulation of T cell receptor expression by CD8(+) lymphocytes in kidney allografts. J. Clin. Invest. 1998; 101:2517–2527. [PubMed: 9616223]
36. Billingham, RE. Free skin grafting in mammals. In: Billingham, RE.; Silvers, WK., editors. Transplantation of Tissues and Cells. Philadelphia: The Wistar Institute Press; 1961. p. 1-24.
37. Coffman T, Geier S, Ibrahim S, Griffiths R, Spurney R, Smithies O, Koller B, Sanfilippo F. Improved renal function in mouse kidney allografts lacking MHC class I antigens. J. Immunol. 1993; 151:425–435. [PubMed: 8326135]
38. Spurney RF, Ibrahim S, Butterly D, Klotman PE, Sanfilippo F, Coffman TM. Leukotrienes in renal transplant rejection in rats. Distinct roles for leukotriene B4 and peptidoleukotrienes in the pathogenesis of allograft injury. J. Immunol. 1994; 152:867–876. [PubMed: 8283057]
39. Spurney RF, Ruiz P, Pisetsky DS, Coffman TM. Enhanced renal leukotriene production in murine lupus: role of lipoxygenase metabolites. Kidney Int. 1991; 39:95–102. [PubMed: 1848329]
40. Wijdenes J, Vooijs WC, Clement C, Post J, Morard F, Vita N, Laurent P, Sun RX, Klein B, Dore JM. A plasmocyte selective monoclonal antibody (B-B4) recognizes syndecan-1. Br. J. Haematol. 1996; 94:318–323. [PubMed: 8759892]
41. Sanderson RD, Lalor P, Bernfield M. B lymphocytes express and lose syndecan at specific stages of differentiation. Cell Reg. 1989; 1:27–35.
42. Hoyer BF, Moser K, Hauser AE, Peddinghaus A, Voigt C, Eilat D, Radbruch A, Hiepe F, Manz RA. Short-lived plasmablasts and long-lived plasma cells contribute to chronic humoral autoimmunity in NZB/W mice. J. Exp. Med. 2004; 199:1577–1584. [PubMed: 15173206]
43. Tedder TF, Engel P. CD20: a regulator of cell-cycle progression of B lymphocytes. Immunol. Today. 15:450–454.
44. Robinson LA, Nataraj C, Thomas DW, Howell DN, Griffiths R, Bautch V, Patel DD, Feng L, Coffman TM. A role for fractalkine and its receptor (CX3CR1) in cardiac allograft rejection. J. Immunol. 2000; 165:6067–6072. [PubMed: 11086038]
45. Ehst BD, Ingulli E, Jenkins MK. Development of a novel transgenic mouse for the study of interactions between CD4 and CD8 T cells during graft rejection. Am. J. Transplant. 2003; 3:1355–1362. [PubMed: 14525595]
46. Epstein MM, Di Rosa F, Jankovic D, Sher A, Matzinger P. Successful T cell priming in B cell-deficient mice. J. Exp. Med. 1995; 182:915–922. [PubMed: 7561694]

47. Mannon RB, Kopp JB, Ruiz P, Griffiths R, Bustos M, Platt JL, Klotman PE, Coffman TM. Chronic rejection of mouse kidney allografts. Kidney Int. 1999; 55:1935–1944. [PubMed: 10231457]
48. Michaels PJ, Fishbein MC, Colvin RB. Humoral rejection of human organ transplants. Springer Semin. Immunopathol. 2003; 25:119–140. [PubMed: 12955463]
49. Bouaziz J-D, Yanaba K, Tedder TF. Regulatory B cells as inhibitors of immune responses and inflammation. Immunol. Rev. 2008; 224:201–214. [PubMed: 18759928]
50. Wu GD, He Y, Chai NN, Toyoda M, Dunn R, Kehry MR, Klein AS, Jordan SC. Anti-CD20 antibody suppresses anti-HLA antibody formation in a HLA-A2 transgenic mouse model of sensitization. Transpl. Immunol. 2008; 19:178–186. [PubMed: 18595710]
51. Patselas T, Marchman W, Araneda D, Thomas J, Thomas F. Normal rejection of xenografts by strongly deficient B-cell animals (X-linked immunodeficient mice). Transplant Proc. 1992; 24:494. [PubMed: 1566401]
52. Cerny A, Ramseier H, Bazin H, Zinkernagel RM. Unimpaired first-set and second-set skin graft rejection in agammaglobulinemic mice. Transplantation. 45:1111–1113.
53. Winn HJ, Baldamus CA, Jooste SV, Russell PS. Acute destruction by humoral antibody of rat skin grafted to mice. J. Exp. Med. 1973; 137:893–910. [PubMed: 4120896]
54. Jooste SV, Winn HJ. Acute destruction of rat skin grafts by alloantisera. J. Immunol. 1975; 114:933–938. [PubMed: 1089727]
55. Russell PS, Chase CM, Winn HJ, Colvin RB. Coronary atherosclerosis in transplanted mouse hearts. II. Importance of humoral immunity. J. Immunol. 1994; 152:5135–5141. [PubMed: 8176230]
56. Nozaki T, Rosenblum JM, Ishii D, Tanabe K, Fairchild RL. CD4 T cell-mediated rejection of cardiac allografts in B cell-deficient mice. J. Immunol. 2008; 181:5257–5263. [PubMed: 18832680]
57. Rifle G, Mousson C, Martin L, Guignier F, Hajji K. Donor-specific antibodies in allograft rejection: clinical and experimental data. Transplantation. 2005; 79:S14–S18. [PubMed: 15699738]
58. Vieira CA, Agarwal A, Book BK, Sidner RA, Bearden CM, Gebel HM, Roggero AL, Fineberg NS, Taber T, Kraus MA, Pescovitz MD. Rituximab for reduction of anti-HLA antibodies in patients awaiting renal transplantation: 1. Safety, pharmacodynamics, and pharmacokinetics. Transplantation. 2004; 77:542–548. [PubMed: 15084932]
59. Claas FH, Doxiadis II. Management of the highly sensitized patient. Curr. Opin. Immunol. 2009; 21:569–572. [PubMed: 19682882]
60. Singh N, Pirsch J, Samaniego M. Antibody-mediated rejection: treatment alternatives and outcomes. Transplant Rev. 2009; 23:34–46.
61. Vo AA, Lukovsky M, Toyoda M, Wang J, Reinsmoen NL, Lai CH, Peng A, Villicana R, Jordan SC. Rituximab and intravenous immune globulin for desensitization during renal transplantation. N. Engl. J. Med. 2008; 359:242–251. [PubMed: 18635429]
62. Stegall MD, Gloor J, Winters JL, Moore SB, Degoey S. A comparison of plasmapheresis versus high-dose IVIG desensitization in renal allograft recipients with high levels of donor specific alloantibody. Am. J. Transplant. 2006; 6:346–351. [PubMed: 16426319]
63. Garrett HE Jr, Duvall-Seaman D, Helsley B, Groshart K. Treatment of vascular rejection with rituximab in cardiac transplantation. J. Heart Lung Transplant. 2005; 24:1337–1342. [PubMed: 16143254]
64. Becker YT, Becker BN, Pirsch JD, Sollinger HW. Rituximab as treatment for refractory kidney transplant rejection. Am. J. Transplant. 2004; 4:996–1001. [PubMed: 15147435]
65. Clatworthy MR, Watson CJ, Plotnek G, Bardsley V, Chaudhry AN, Bradley JA, Smith KG. B-cell-depleting induction therapy and acute cellular rejection. N. Engl. J. Med. 2009; 360:2683–2685. [PubMed: 19535812]

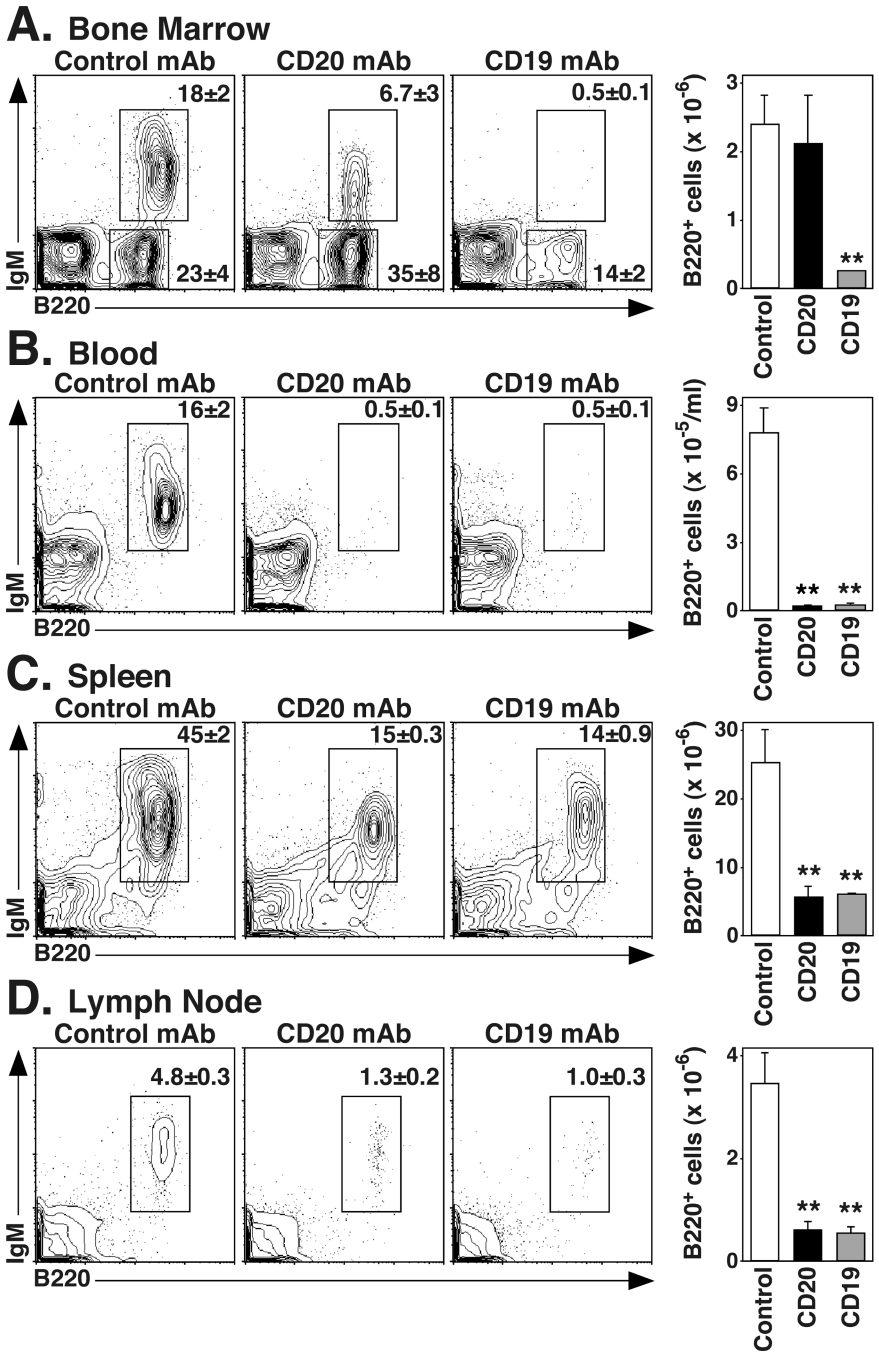

Figure 1.

CD20 and CD19 mAbs effectively deplete mature B cells *in vivo*. C57BL/6–129 huCD19Tg mice were given control, CD20, or CD19 mAb. B cell numbers within the (**A**) BM, (**B**) blood, (**C**) spleen, and (**D**) pooled inguinal, axial, and brachial LN were analyzed 7 d later by immunofluorescence staining with flow cytometry analysis. Representative dot plots are shown, with the mean (± SEM) percentage of $B220^+IgM^+$ or $B220^+IgM^-$ cells indicated. Bar graphs indicate the mean (± SEM) numbers of $B220^+$ B cells contained within each tissue after the indicated treatment (n=3 mice per group) from one of two independent

experiments. Significant differences between control and CD20 or CD19 mAb-treated sample means are indicated: **, $p<0.01$.

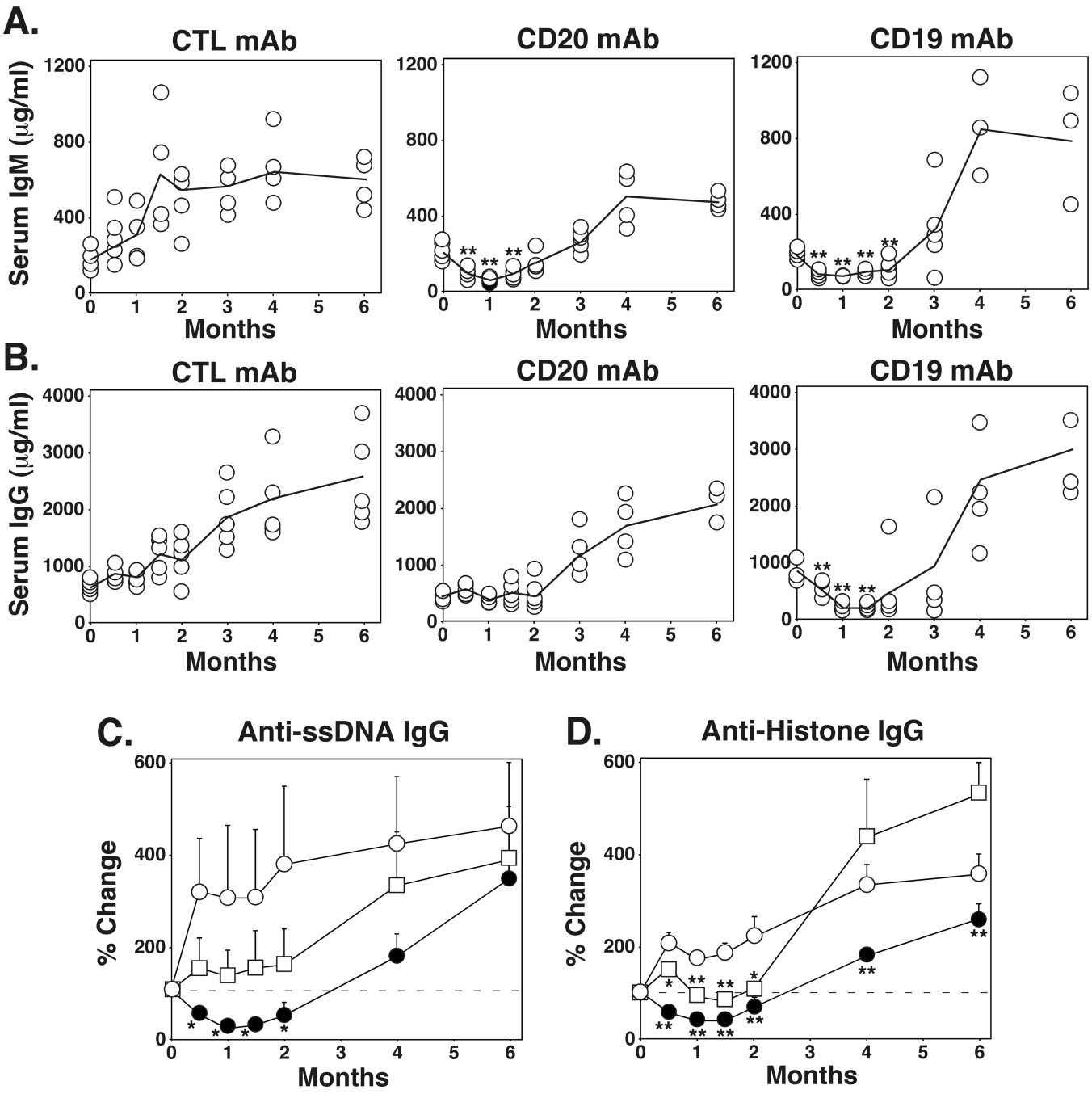

Figure 2.

CD19 mAb treatment depletes serum IgG, while CD20 mAb treatment does not. Two mo-old C57BL/6 huCD19Tg mice were given control, CD20, or CD19 mAb on day 0, with serum harvested at the indicated time points for analysis by ELISA. (**A-B**) Values represent serum IgM (A) and IgG (B) concentrations from individual mice receiving the indicated mAb. Solid lines connect mean serum Ig concentrations for each group. Significant differences between sample means relative to day 0 are indicated: **, p<0.01. (**C-D**) Values represent the mean (± SEM) percentage changes in relative ODs for ssDNA-specific (C) or histone-specific (D) IgG from individual sera relative to day 0 values within the indicated treatment groups (n=4–5 mice per group). All values were normalized to 0 for day 0, with

horizontal dashed lines indicating 100% values. Significant differences between sample means relative to the control mAb treatment group are indicated: *, $p<0.05$; **, $p<0.01$.

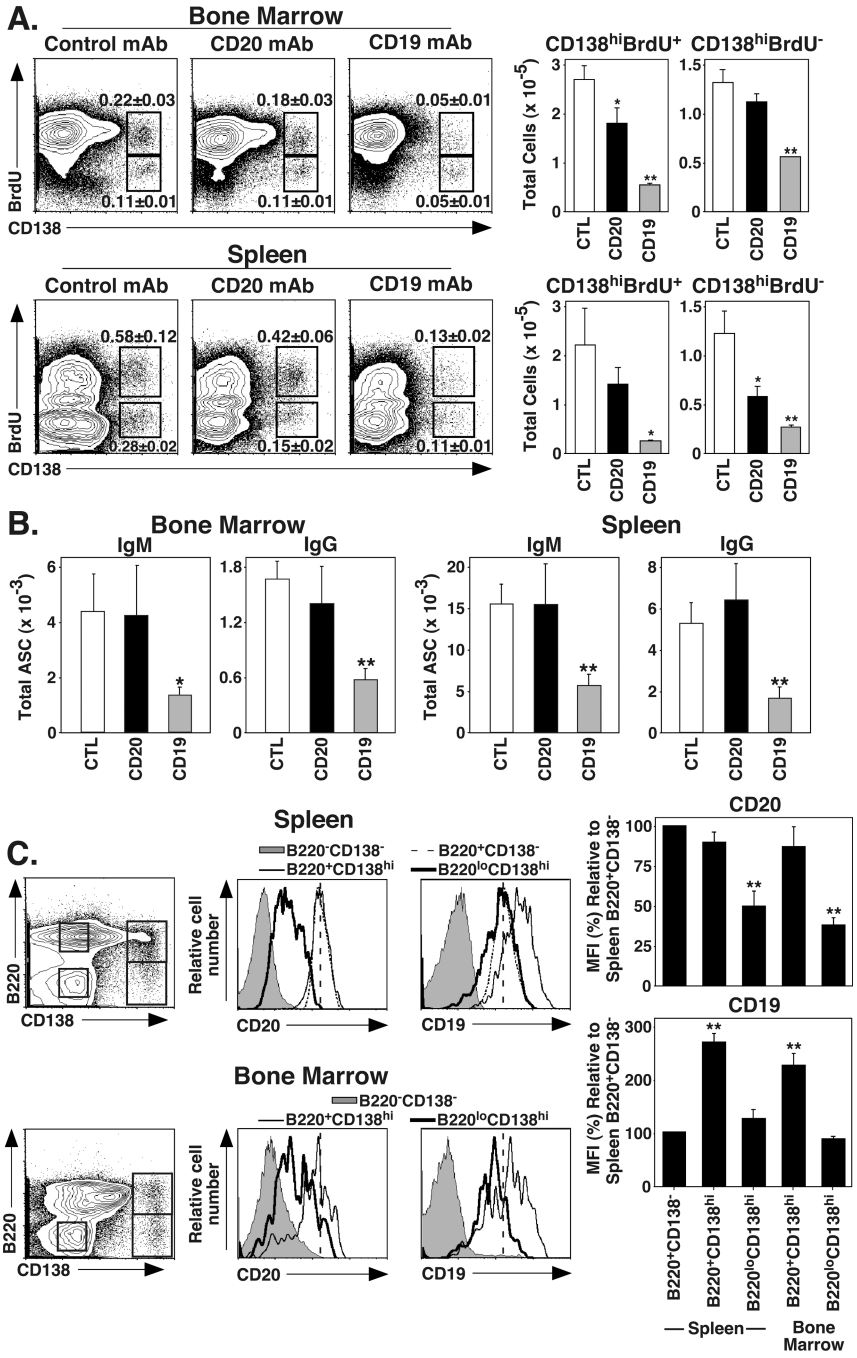

Figure 3.

CD19 mAb treatment depletes Ab-secreting plasma cells. (**A**) CD19 mAb depletes both short-lived and long-lived CD138^{hi} plasma cells. C57BL/6–129 huCD19Tg mice were fed BrdU for 7 d prior to and following control, CD20, or CD19 mAb treatments, with BM and spleen cells analyzed for surface CD138 and intracellular BrdU staining on day 7. Dot plots show mean (± SEM) percentages of CD138^{hi}BrdU^{+} (short-lived plasma cells) and CD138^{hi}BrdU^{-} (long-lived plasma cells). Bar graphs indicate mean numbers of CD138^{hi}BrdU^{+} and CD138^{hi}BrdU^{-} cells from mice receiving the indicated treatment (n=8 mice per group). (**B**) C57BL/6 huCD19Tg mice were given control, CD20, or CD19 mAb,

with BM and spleen Ab-secreting cell (ASC) numbers determined 7 d later by ELISPOT analysis. Bar graphs indicate mean (± SEM) numbers of IgM and IgG ASCs (n=4 mice per group). (**C**) CD19 expression is maintained on $CD138^+$ plasmablasts, while CD20 expression decreases. BM and spleen cells from naive C57BL/6–129 huCD19Tg mice were co-stained for CD138, B220, CD20, and CD19. Representative dot plots (left panels) indicate the $B220CD138^-$, $B220^+CD138^-$, $B220^+CD138^{hi}$, and $B220^{lo}CD138^{hi}$ cell populations that were analyzed for CD20 and CD19 expression (right panels). Vertical dashed lines indicate the MFI of CD20 or CD19 expression by splenic $B220^+CD138^-$ B cells. Bar graphs indicate mean (± SEM) levels of CD20 or CD19 expression relative to spleen $B220^+CD138^-$ B cells. Background staining MFI values (<10) were subtracted from each respective population before normalization to splenic $B220^+CD138^-$ cells. Results from 3 individual experiments (n=3 mice in each experiment) were pooled. (A-C) Significant differences between sample means relative to the control mAb treatment (A-B) or to the $B220^+CD138^-$ population (C) are indicated: *, $p<0.05$; **, $p<0.01$.

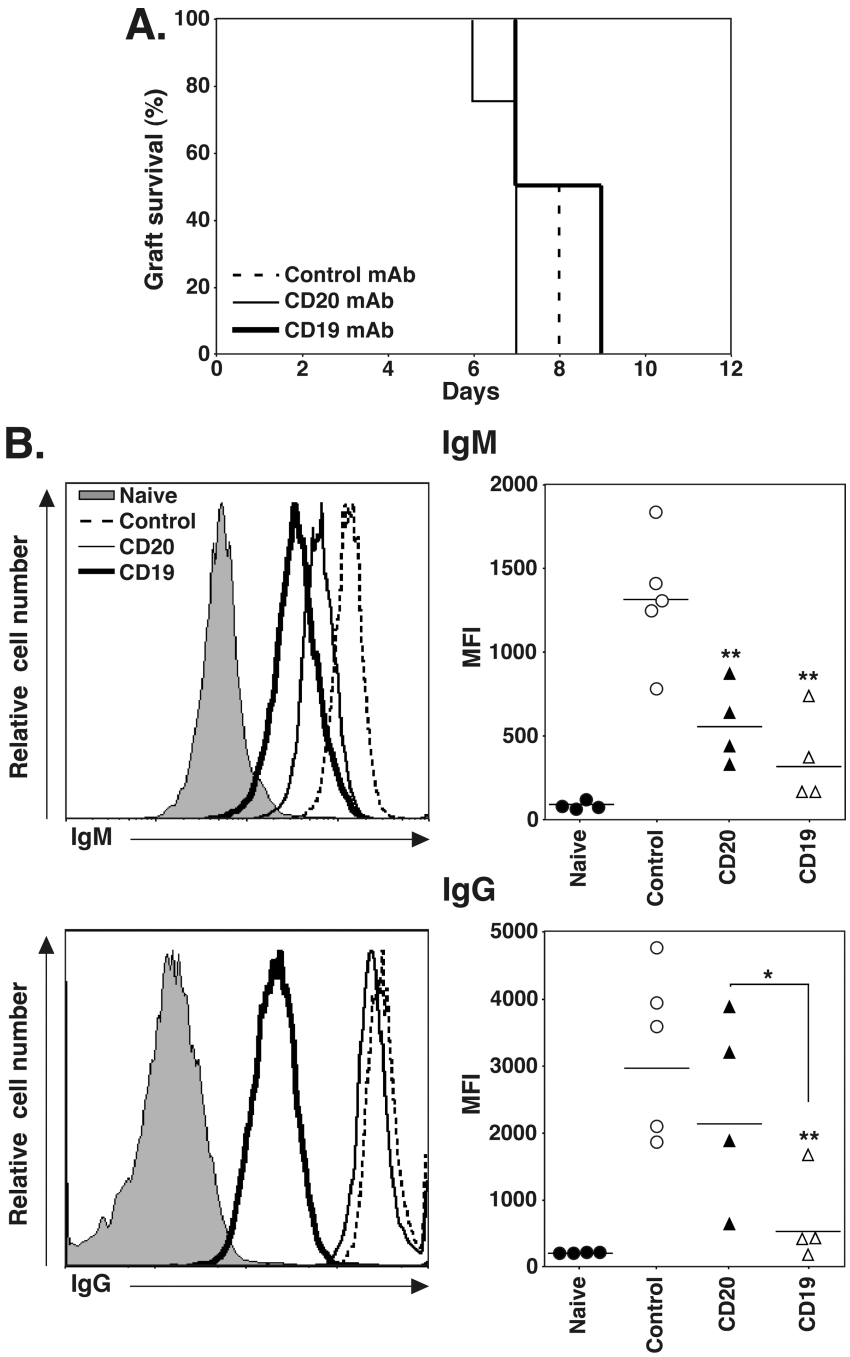

Figure 4.

CD19 mAb treatment impairs allograft-specific IgG production. C57BL/6–129 huCD19Tg mice were given control, CD20, or CD19 mAb 7 d before receiving a fully MHC-mismatched DBA/2 heterotopic cardiac allograft. (**A**) Allograft survival following control (n=5, dashed line), CD20 (n=4, solid line), or CD19 (n=4, heavy solid line) mAb treatment. (**B**) Serum was collected from mice in (A) 14 d after grafting and analyzed for DBA/2-specific IgM (top panels) and IgG (bottom panels) by indirect immunofluorescence staining with flow cytometry analysis. Flow cytometry histograms (left panels) show representative IgM and IgG staining of DBA/2-derived P815 cells with serum from control (dashed line),

CD20 (solid line), and CD19 (heavy solid line) mAb-treated mice, and untransplanted naïve mice (shaded). Values (right panels) represent the MFI of stained cells from individual mice that received the indicated treatment. Horizontal bars indicate mean MFI values for each group. Significant differences between control and CD20 or CD19 mAb sample means, or between specified means, are indicated: *, $p<0.05$; **, $p<0.01$.

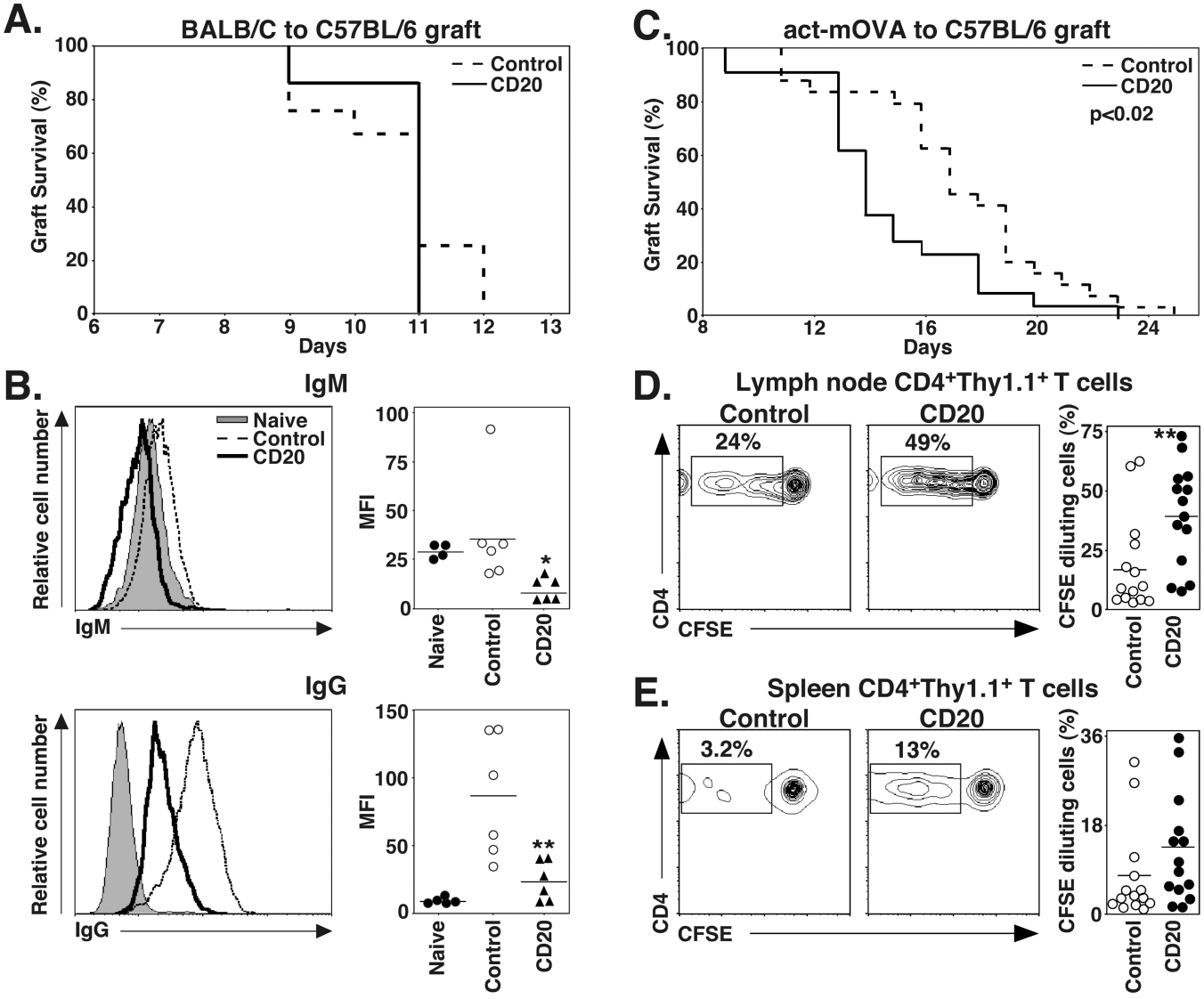

Figure 5.

CD20 mAb treatment impairs allograft-specific IgG generation, but accelerates minor histocompatibility-mismatched skin allograft rejection and alloAg-specific $CD4^+$ T cell proliferation. (**A**) C57BL/6 mice were given control or CD20 mAb 7 d before receiving BALB/C skin allografts. The graph shows allograft survival following control (dashed line; n=12) and CD20 (solid line; n=7) mAb treatment. (**B**) Serum was collected from mice in (A) 14 d after grafting and analyzed for BALB/C-specific IgM (top panels) and IgG (bottom panels) by indirect immunofluorescence staining with flow cytometry analysis. Flow cytometry histograms (left panels) show representative IgM and IgG staining of BALB/C-derived AG8 cells with serum from control (dashed line) and CD20 (solid line) mAb-treated mice, and untransplanted naïve (shaded) mice. Values (right panels) represent the MFI of stained cells from individual mice. Horizontal bars indicate mean MFI values for the group. (**C**) C57BL/6 mice were given control or CD20 mAb 7 d before receiving skin allografts from act-mOVA transgenic mice. The graph shows allograft survival following control (dashed line; n=24) and CD20 (solid line; n=21) mAb treatment. (**D-E**) C57BL/6 mice were given control or CD20 mAb 6 d before receiving CFSE-labeled $Thy1.1^+CD4^+$ T cells from OT-II mice. One d later, the mice received Act-mOVA skin grafts. (D) Draining LN and (E)

spleen lymphocytes were isolated 5 d later, with CD4 expression and CFSE dilution of $Thy1.1^+$ T cells assessed by immunofluorescence staining with flow cytometry analysis. Representative CFSE versus cell surface CD4 staining for $Thy1.1^+$ cells is shown, with the percentages of CFSE-diluted $CD4^+$ cells within each gate indicated as a fraction of total $CD4^+$ $Thy1.1^+$ T cells. Values (right panels) represent the percentage of CFSE-diluted cells from individual control mAb- and CD20 mAb-treated mice. Horizontal bars indicate mean values for groups. Significant differences between control mAb and CD20 mAb sample means are indicated: *, $p<0.05$; **, $p<0.01$.

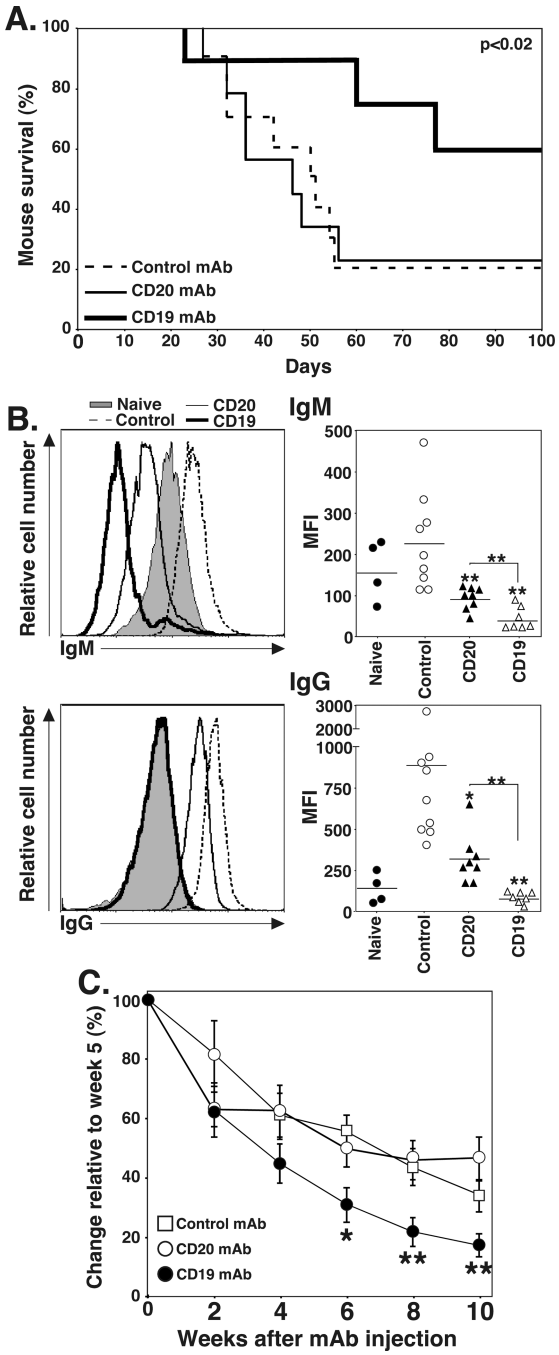

Figure 6.

CD19 mAb treatment prevents renal allograft rejection, impairs allograft-specific IgG generation, and reduces pre-existing serum IgG levels. C57BL/6–129 huCD19Tg mice were given control, CD20, or CD19 mAb 7 d before receiving a DBA/2 renal allograft. A nephrectomy was performed on the remaining kidney 1–3 d following allografting, and mouse survival was monitored daily as a measure of allograft rejection. (**A**) Allograft survival following control (n=9, dashed line), CD20 (n=8, solid line), or CD19 (n=7, heavy solid line) mAb treatments. (**B**) Serum was collected from mice 21 d after grafting and analyzed for DBA/2-specific IgM (top panels) and IgG (bottom panels) by indirect

immunofluorescence staining with flow cytometry analysis. Flow cytometry histograms (left panels) show representative IgM and IgG staining of P815 cells with serum from control (dashed line), CD20 (solid line), and CD19 (heavy solid line) mAb-treated mice, and untransplanted naïve (shaded) mice. Values (right panels) represent the results from individual mice that received the indicated treatment. Horizontal bars indicate mean MFI values for groups. (**C**) C57BL/6–129 huCD19Tg mice were immunized with DBA/2 splenocytes at week 0 and boosted at week 2. Mice were then randomized and given control, CD20, or CD19 mAb at week 5. Serum was harvested at the indicated time points, with DBA/2-specific IgG measured by indirect immunofluorescence staining with flow cytometry analysis. Values represent the mean percent change in MFI relative to week 5 (n=4–5 mice per group). Significant differences between control and CD20 or CD19 mAb sample means, or between specified means, are indicated: *, $p<0.05$; **, $p<0.01$.

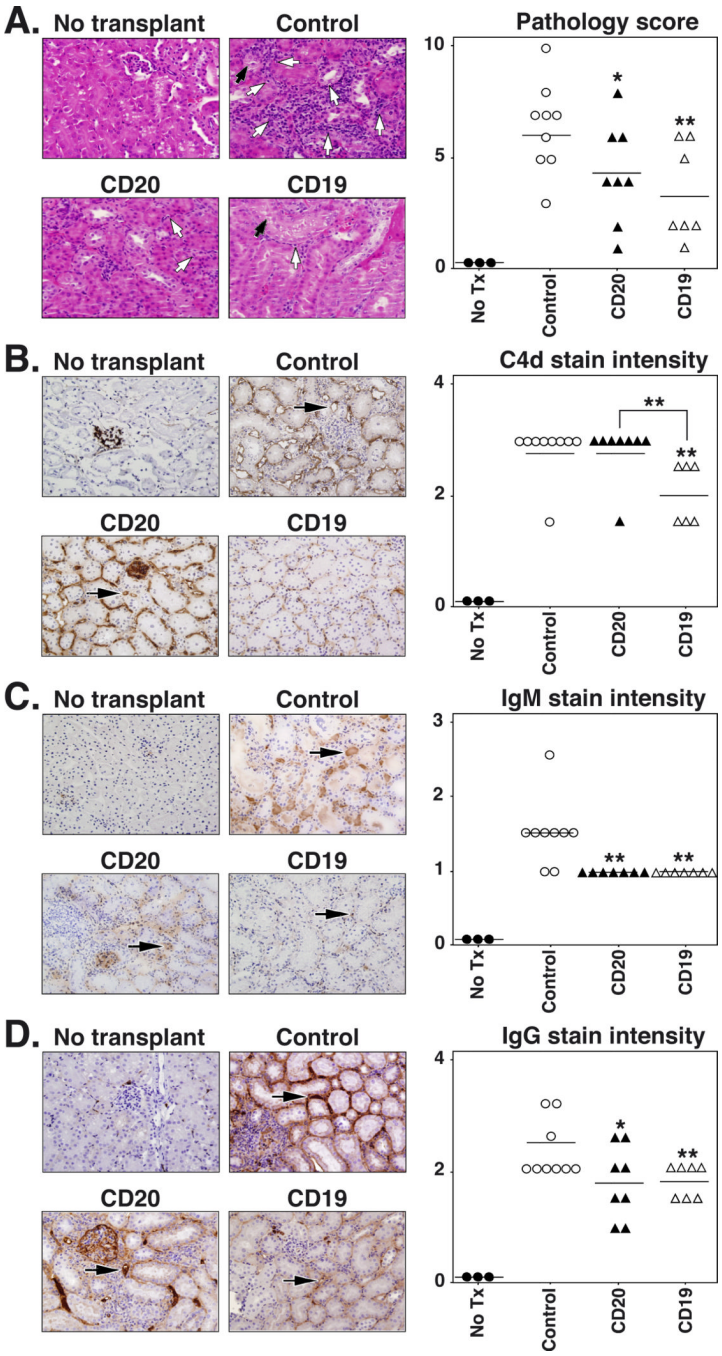

Figure 7.

CD19 mAb treatment reduces renal injury and C4d deposition following renal allografting. C57BL/6–129 huCD19Tg mice were given control, CD20, or CD19 mAb 7 d before receiving a fully MHC-mismatched DBA/2 renal allograft as in figure 6. Mice were sacrificed 21 d after grafting for donor kidney analysis. (**A**) Representative H&E stained samples (left panels), with tubulitis (white arrows) and foci of acute tubular necrosis (black arrows) indicated. Histopathologic scores (right panel) for individual kidneys from mice that received the indicated treatments. Horizontal bars indicate mean overall scores for each group. (**B-D**) Kidney sections (left panels) from mice treated as in (A) were stained for C4d

(B), IgM (C), and IgG (D) deposition, with representative samples shown. Black arrows indicate representative peritubular capillaries. (Right panel) Values represent the staining intensity score for peritubular capillaries from individual kidneys of mice that received the indicated treatment. Horizontal bars indicate mean score values for the group. Significant differences between control and CD20 or CD19 mAb sample means, or between specified means, are indicated: *, $p<0.05$; **, $p<0.01$.

Table I

B cell subsets in CD20 and CD19 mAb-treated mice[a]

Tissue	Subset[b]	Control mAb[c]	CD20 mAb	CD19 mAb
BM	$B220^+$	2.04 ± 0.34	1.80 ± 0.60	0.21 ± 0.02 **,#
	Pro	0.44 ± 0.05	0.47 ± 0.01	0.40 ± 0.07
	Pre	0.81 ± 0.23	1.12 ± 0.43	0.05 ± 0.01 *,#
	Immature	0.57 ± 0.10	0.31 ± 0.13	0.006 ± 0.002 **,#
	Mature	0.38 ± 0.07	0.01 ± 0.005 **	0.004 ± 0.001 **
Blood	$B220^+$	7.86 ± 1.09	0.18 ± 0.05	0.22 ± 0.09
Spleen	$B220^+$	23.93 ± 4.58	5.30 ± 1.50 **	5.63 ± 0.17 **
	T1	3.39 ± 0.42	1.40 ± 0.45 *	0.78 ± 0.04 **
	T2	3.01 ± 0.38	0.04 ± 0.02 **	0.57 ± 0.12 **
	Marginal zone	3.15 ± 0.54	0.28 ± 0.10 **	0.87 ± 0.17 **
	Mature	16.16 ± 3.78	3.79 ± 0.93 **	3.73 ± 0.31 **
LN	$B220^+$	0.37 ± 0.06	0.06 ± 0.02 **	0.05 ± 0.01 **

[a] Naïve huCD19Tg mice were treated with control, CD20, or CD19 mAb, with B cell subset numbers determined by immunofluorescence staining with flow cytometry analysis.

[b] B cell subsets were: BM pro-B ($B220^{low}IgM^-CD43^+$), pre-B ($B220^{low}IgM^-CD43^-$), immature B ($B220^{low}IgM^+$), and mature B ($B220^{high}IgM^+$); spleen mature ($B220^+CD24^+CD21^+$), T1 ($B220^+CD24^{high}CD21^-$), T2 ($B220^+CD24^{high}CD21^+$), and marginal zone ($B220^+CD21^{high}CD1d^+$).

[c] Values (± SEM) indicate cell numbers ($\times 10^{-6}$) present in each tissue 7 d after mAb treatment (n=3 mice per group): blood shown as cells $\times 10^{-5}$/ml, LN as pooled bilateral inguinal, axial, and brachial LN, and BM as pooled femurs. Significant differences between means are indicated:

* $p \leq 0.05$ vs. control group;

** $p \leq 0.01$ vs. control group;

$p \leq 0.05$ vs. CD20 mAb-treated group.

Table II

Kidney pathology

	Control mAb	CD20 mAb	CD19 mAb
Tubulitis	1.4 ± 0.20	0.88 ± 0.01 *	0.43 ± 0.18 **,#
Interstitial inflammation	2.2 ± 0.17	1.5 ± 0.01 **	1.29 ± 0.16 **
Glomerulitis	0.56 ± 0.20	0.38 ± 0.18	0.29 ± 0.16
Arteritis	0.89 ± 0.35	0.50 ± 0.19	0.29 ± 0.16
Interstitial fibrosis	0.67 ± 0.19	0.63 ± 0.18	0.86 ± 0.13
Tubular atrophy	0.56 ± 0.20	0.38 ± 0.18	0 ± 0 **,#
Total score	6.4 ± 0.67	4.4 ± 0.80 *	3.4 ± 0.81 **

Naïve huCD19Tg mice were treated with control, CD20, or CD19 mAb as in figure 7 before receiving a DBA/2 kidney allograft. After 21 d, the mice were euthanized and a portion of the transplanted kidney was removed and placed in 10% buffered formalin. After formalin fixation, kidney tissue sections were stained with H&E, PAS, and Masson's Trichrome. Slides were scored for renal injury based on the following scale: 0, no abnormalities; 1, mild; 2, moderate; and 3, severe. Values represent the mean (± SEM) pathological score for the indicated parameter. Significant differences between sample means are indicated:

* $p \leq 0.05$ vs. control mAb group;

** $p \leq 0.01$ vs. control mAb group;

# $p < 0.05$ vs. CD20 mAb group.